Proceedings of The Magnetized Plasma in Galaxy Evolution
Sep. 27th – Oct. 1st 2004, Jagiellonian University, Kraków, Poland
Eds. K.T. Chyży, K. Otmianowska-Mazur, M. Soida and R.-J. Dettmar

The magnetic field along the jet of NGC 4258* and its interaction with molecular gas

Marita Krause[1], A. Löhr[1], C. Fendt[2], and N. Neininger[3]

[1] Max-Planck-Institut für Radioastronomie, Auf dem Hügel 69, 53121 Bonn, Germany
[2] Max-Planck-Institut für Astronomie, Königstuhl 17, 69117 Heidelberg, Germany
[3] Radioastronomisches Institut der Universität Bonn, Auf dem Hügel 71, 53121 Bonn, Germany

Abstract

We observed NGC4258 in radio continuum and linear polarization with a high resolution of $2\overset{''}{.}2 \times 2\overset{''}{.}4$ HPBW with the VLA in C-configuration at 3.6 cm. The radio jets are well visible and the northern jet is linearly polarized. The magnetic field orientation is mainly along the jet direction with indications for an additional toroidal field component or a helical magnetic field around the jet axis. The equipartition field strength is about $300\,\mu$G for a relativistic electron-proton jet and $\simeq 100\,\mu$G for a relativistic electron-positron jet.

With observations of molecular gas (12 CO(1-0)) with the IRAM interferometer at Plateau de Bure we detected two parallel CO ridges along the jets. It looks like a tunnel with walls made of molecular gas. We propose that the concentration of CO just along these ridges is due to an interaction of the rotating gas clouds in the disk of NGC 4258 with the magnetic field of the jets.

1 Introduction

Many spiral galaxies host nuclear jets. These are weak and small compared to those of radio galaxies and quasars and may be best detected by their interaction with the ISM. The jets are expected to emerge perpendicular to the nuclear accretion disk. Hence, only if the nuclear accretion disk has a significant tilt with respect to the galaxy's plane, the jets travel a long way through the ISM and are well observable. Such a geometry was first proven for NGC 4258 by observations of the water maser emission from the accretion disk (Greenhill et al. 1995). The accretion disk has an inclination angle of 83° and a position angle (p.a.) of 86°, i.e. it is oriented nearly east-west. The p.a. of the galactic disk, however, is 150°, which is nearly north-south, and its inclination is 72° (van Albada 1980). Thus, the plane of the galactic disk and the plane of the accretion disk have a significant angle to each other. As the jets emerge perpendicular to the accretion disk, they have to pass the galactic disk at a rather small angle. Due to the projection of the whole system with respect to the Earth, the inner projected jet direction is almost parallel to the major axis of the galactic disk.

*Based on observations with the 100-m telescope of the MPIfR (Max-Planck-Institut für Radioastronomie) at Effelsberg

2 Radio continuum

2.1 Observations

To further investigate the jet geometry and especially the magnetic field along the jets we obtained data with the Very Large Array (VLA)[1] at $\lambda 3.6$ cm (8.44 Ghz) and compared these with reprocessed VLA data by Hummel et al. (1989) at $\lambda 6.2$ cm (4.86 GHz) and with observations at $\lambda 2.8$ cm (10.55 GHz) made with the Effelsberg 100-m telescope. The observations and data reduction have been extensively described by Krause & Löhr (2004). The highest resolution map at 8.44 GHz has $2\overset{''}{.}2 \times 2\overset{''}{.}4$ HPBW and an rms noise of 8 μJy/b.a.. This map was superimposed on the Hα map of the galaxy observed at the Hoher List Observatory of the University of Bonn and is shown in Fig.1. Maps even more sensitive to weak extended structures and the polarized emission were made with natural weights at the expense of a slightly lower HPBW of $2\overset{''}{.}9 \times 3\overset{''}{.}3$ with an rms noise of 8 μJy/b.a. in total intensity and 7 μJy/b.a. in linear polarization.

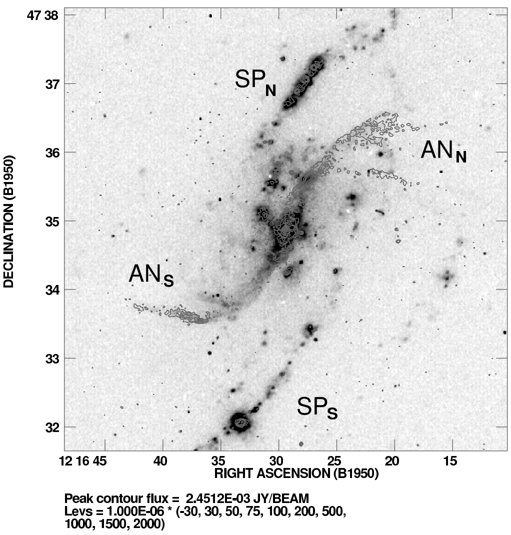

Figure 1: The 8.44 GHz high resolution (HPBW $= 2\overset{''}{.}2 \times 2\overset{''}{.}4$) map in total intensity as obtained with the VLA C-configuration superimposed on the Hα map of the galaxy observed at the Hoher List Observatory of the University of Bonn. The normal spiral arms are marked as SP_N and SP_S, the anomalous arms as AN_N and AN_S.

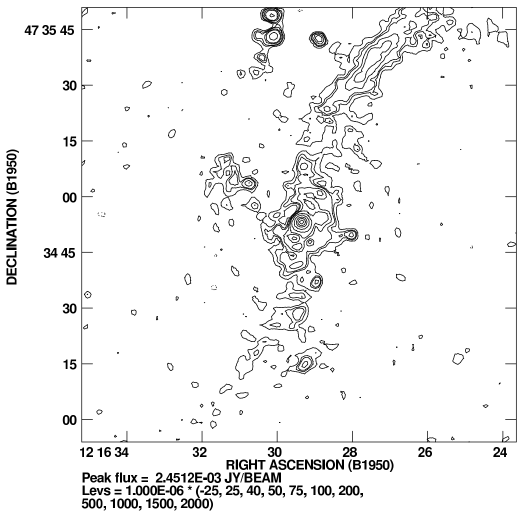

Figure 2: The 8.44 GHz high resolution (HPBW $= 2\overset{''}{.}2 \times 2\overset{''}{.}4$) map detail of the central region in total intensity. The r.m.s. noise is 8 μJy/b.a..

[1]The VLA is a facility of the National Radio Astronomy Observatory. The NRAO is operated by Associated Universities, Inc., under contract with the National Science Foundation.

2.2 Results

2.2.1 Jet geometry

The total intensity at 8.44 GHz in the central region (4×4)kpc is shown in Fig.2. From our observations we determined the position angle of the jet up to a distance of $24''$ from the nucleus to be p.a. $= -3° \pm 1°$. This is in full agreement with the value given by Cecil et al. (2000) from their radio observations and along the projected spin axis of the accretion disk as determined by Miyoshi et al. (1995).

At larger distances from the nucleus the jets change their direction from a north-south orientation to northwestern to southeastern symmetrically on both sides at a projected distance of $24''$ from the galactic center to p.a. $= -43° \pm 1°$.

2.2.2 Polarized intensity

In the natural weighted maps we obtained linearly polarized intensity at a resolution of $2\farcs9 \times 3\farcs3$ HPBW. This is the first time that extended linear polarization has been detected in NGC 4258 with arcsec resolution. The polarized intensity has been detected exclusively at the center and along the jets. Whereas the degree of linear polarization (polarized intensity/total intensity) at the center is small and at least partly instrumental, that one along the northern jet lies between 35% and 65%.

2.2.3 Faraday rotation and magnetic fields

The observed electric vectors are rotated by Faraday effects. We determined the rotation measure RM between $\lambda 3.6$ cm and $\lambda 6.2$ cm at $14''$ HPBW. The calculated RM varies between 400 and 800 rad/m^2. The nπ ambiguity (i.e. the RM value that corresponds to a Faraday rotation of n180° and hence is undistinguishable by observations at only two wavelengths) between these two wavelengths is as high as 1216 rad/m^2 for n=1. A substraction of one 180° rotation (n=-1) from these values leads to RM between -800 and -400 rad/m^2 which is in absolute value not distinguishable from the values above.

We tried to solve the RM ambiguity using the $\lambda 2.8$ cm observations. Therefore we smoothed the $\lambda 3.6$ cm map out to $69''$ HPBW, the angular resolution of the $\lambda 2.8$ cm map. The vectors between $\lambda 2.8$ cm and $\lambda 3.6$ cm rotate *clockwise* by about 40–80° which correspond to negative RM between about -1500 and -3000 rad/m^2. We conclude that the vectors rotate further clockwise towards the E-vectors observed at $\lambda 6.2$ cm. This corresponds to negative RM values. Hence we consider the values for n=1 between $\lambda 3.6$ cm and $\lambda 6.2$ cm as more probable, i.e.the corresponding RM ranges from -800 to -400 rad/m^2. A more detailed discussion about the Faraday rotation and depolarization effects can be found in Krause & Löhr (2004).

The galactic foreground rotation measure is negligible towards the direction of this galaxy (Krause et al. 1984), hence the observed RM is exclusively associated with NGC 4258. With our RMs we corrected the E-vectors for Faraday rotation. The resulting magnetic field orientation is shown in Fig. 3 superimposed on the smoothed $\lambda 3.6$ cm map. The vectors generally follow the jet direction, also along the main bifurcation of the northern jet. They are, however, somewhat tilted with respect to the jet direction. We infer that the magnetic field is mainly poloidal along the jet axis with a (weaker) toroidal component. This can be a superposition of a poloidal and (weaker) toroidal magnetic field in different layers around the jet axis or is consistent with a slightly helical magnetic field around the jet axis.

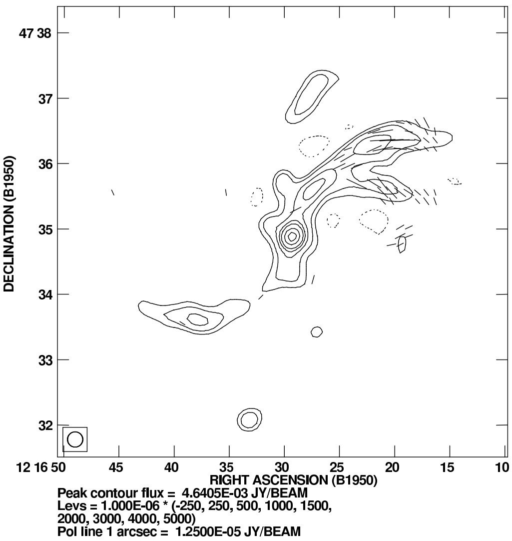

Figure 3: The 8.44 GHz map of the total intensity (HPBW $= 14''$). The r.m.s. noise is 70 μJy/b.a. The B-vectors show the magnetic field direction with their length proportional to the polarized intensity.

For this magnetic field geometry we calculated the magnetic field strengths from the high resolution map for the northern jet assuming energy equipartition between the magnetic field and the relativistic particles. We used a nonthermal spectral index of $\alpha_{\rm n} = -0.65 \pm 0.10$ along the jets (Hyman et al. 2001) and assumed $L = 50$ pc as line of sight through the jet. For an assumed electron-proton jet ($K = 100$, Krause et al. 1984, Beck & Krause, in prep.) we estimated a magnetic field strengths of 310 ± 15 μG for the total field and 250 ± 25 μG for the uniform field and magnetic field strengths of 90 ± 5 μG, resp. 70 ± 10 μG for an assumed electron-positron jet (K=1).

3 Molecular lines

3.1 Observations

We observed the central region of NGC 4258 along the inner Hα jets up to a radial distance of about 2 kpc in ^{12}CO(1-0) using the Plateau de Bure (PdB) interferometer in its compact configuration. We made a mosaic consisting of 5 fields that were aligned with the CO ridge known from previous single-dish observations (Krause et al. 1990) and covered an area of $100'' \times 40''$ with a uniform sensitivity along the major axis of the oval.

We corrected the data for 'missing short spacings' by combining them with single dish data obtained with the 30-m telescope at Pico Veleta by Cox & Downes (1996). For the combination we used the 'ssc method' as described by Weiss et al. (2001) that works on the finally reduced (cleaned and corrected for primary beam attenuation) interferometer cube. The angular resolution of the final maps is $4\overset{''}{.}6 \times 3\overset{''}{.}3$ with a position angle of $31°$.

3.2 Results

We determined the zero moments by integrating the line intensity in the individual spectra. All points with values below 3 times the noise level ($\sigma = 0.7\,{\rm Jy/beam\,km\,s^{-1}}$) of the inner

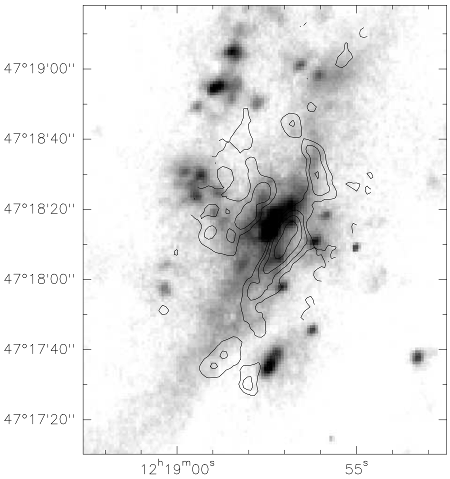

Figure 4: Contours of the integrated intensity of ^{12}CO(1-0) of NGC 4258 superimposed on the central part of the Hα image of the galaxy from Fig. 1. The rms-noise in the inner part of the map is 0.7 Jy/beam km s^{-1}. The contour levels are 2, 4, 10, 20, 35, 50 Jy/beam km s^{-1}. The normal spiral arms are located in the north and south.

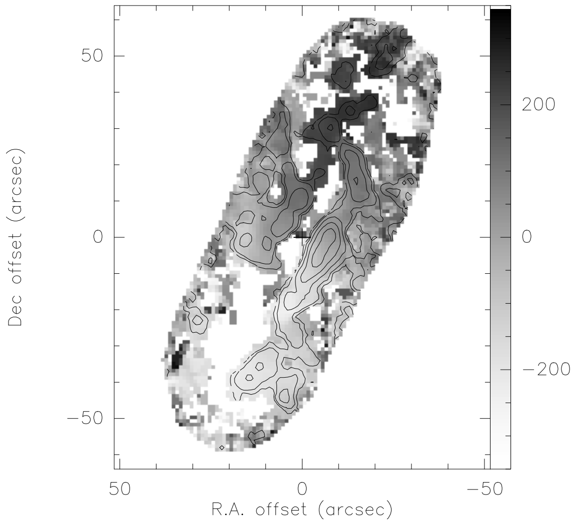

Figure 5: Isovelocity map of ^{12}CO(1-0) of NGC 4258 with respect to the systemic velocity. All points for which the integrated intensity is below its 3σ noise level are discarded. The contours represent the integrated intensity and are equal to those in Fig. 4.

part of the map were discarded in the calculation. The spatial distribution of the integrated CO in the observed area is shown in Fig. 4 as contours.

The molecular gas follows *two* parallel ridges along a position angle of about $-25°$. The western rigdge is stronger in intensity and with a total projected length of about $80''$ more extended than the eastern one. The width of each ridge (HPBW) is about $7''$ (250 pc) and the width of the CO depleted region between them is about $5''$ (175 pc). The orientation of the ridges agrees well with previous CO observations. The integrated ^{12}CO(1-0) intensity is superimposed on the Hα image of the galaxy in Fig. 1. The ridges follow the Hα distribution but are more extended. The Hα has its maximum in between the two CO ridges with a slight shift towards the stronger western ridge. The Hα emission however is broader than the CO emission and outlines the jet to larger distances from the nucleus. Contrary to previous interpretations of Plante et al. (1991 and 1994) the CO does not outline 'walls' around the Hα jets and hence does not confine it. It rather seems to be mixed in location and in velocity with the Hα gas.

Assuming the "standard" $N(H_2)/I_{CO}$ conversion factor of $2.3 \cdot 10^{20}$ mol cm^{-2} (K km/s)$^{-1}$ (Strong et al. 1988) we derive from the integrated ^{12}CO(1-0) intensity a mass of molecular hydrogen of $M_{H_2} \simeq 10^9\ M_\odot$.

Fig. 5 shows the iso-velocity map with respect to the systemic velocity. All points for which the integrated intensity is below its 3σ noise level were discarded. The velocities in the southern part of NGC 4258 have blue shifted velocities whereas those in the northern part are red shifted up to about $\pm$ 200 km s^{-1} as expected for gas in normal galactic rotation. Also the p-v diagramm along the CO ridge and the huge amount of molecular gas that seems to be involved supports the view that the molecular gas is disk gas in normal galactic rotation.

However, we observe a significant velocity gradient between the two ridges at the same distance from the nucleus resp. which is quite unusual. The velocity shift between the two ridges is about 50 $\mathrm{km\,s^{-1}}$.

This strange velocity shift, the existence of the two ridges and the *non-detection* of CO outside the region along the inner jets can be explained by an interaction of the molecular gas with the jets where the jets passes the molecular disk. We propose that the rotating gas clouds are *coupled by ambipolar diffusion with the magnetic field* of the current-carrying jets. We estimated the kinematic time scales for the jet itself, the jet-cloud interaction on one hand and dynamical time scales of molecular clouds and the ambipolar diffusion on the other (Krause, Fendt, Neininger, in prep.). We conclude that the proposed interaction is quite feasible from a theoretical point of view. This magnetic interaction is thought to increase the residence time of the molecular clouds near the jets in comparison with other loci in the galactic disk and hence lead to the quasistatic CO ridge.

References

van Albada, G.D., 1980, A&A, 90, 123

Cecil, G., Greenhill, L. J., DePree, C. G., et al., 2000, ApJ, 536, 675

Greenhill L.J., Jiang D.R., Moran J.M., Reid M.J., 1995, ApJ, 440, 619

Hyman, S. D., Calle, D., Weiler, K. W., et al., 2001, ApJ, 551, 702

Hummel E., Krause M., Lesch H., 1989, A&A, 211, 266

Krause M., Löhr A., 2004, A&A, 420, 115

Krause M., Cox P., Garcia-Barreto J.A., Downes D., 1990, A&A, 233, L1

Krause, M., Beck, R., & Klein U., 1984, A&A, 138, 385

Miyoshi, M., Moran, J., Herrnstein, J. R., et al., 1995, Nature, 373, 127

Plante R.L., Lo K.Y., Roy J-R., Martin P., Noreau L., 1991, ApJ 381, 110

Plante R.L., Handa T., Lo K.Y., 1994, in: Ishiguro M., Welch W.J. (ed), Astronomy with millimeter and submillineter wave interferometry, IAU Colloquium 140, A.S.P. Conf.Ser. Vol. 59, p. 359

Strong A.W., Bloemen J.B.G.M., Dame, T.M., Grenier I.A., Hermsen W., Lebrun F., Nyman L.-Å., Pollock A.M.T., Thaddeus P., 1988, A&A 207, 1